Sodium chloride assists copper release, enhances antibacterial efficiency, and introduces atmospheric corrosion on copper surface

Jiaqi Luo, Christina Hein, Jean-François Pierson, Frank Mücklich

Sodium chloride assists copper release, enhances antibacterial efficiency, and introduces atmospheric corrosion on copper surface

Jiaqi Luo[a,b,*], Christina Hein[c], Jean-François Pierson[b], Frank Mücklich[a]

[a] Functional Materials, Saarland University, 66123 Saarbruecken, Germany

[b] Université de Lorraine, CNRS, IJL, F-54000 Nancy, France

[c] Inorganic Solid State Chemistry, Saarland University, 66123 Saarbruecken, Germany

[*] Email address: jiaqi.luo@uni-saarland.de

Abstract

Sodium chloride (NaCl) is commonly found in the physiological buffers. This study found out its additional but important role in antibacterial efficiency test by better corroding metallic copper surface. Combined with multiple characterisation methods including scanning electron microscope, grazing incidence X-ray diffractometer, and inductively coupled plasma mass spectrometry, 0.9% saline was observed to cause localised corrosion attacks on copper surface, enhancing release of copper content. The 1 h killing rate against *Escherichia coli* was thus promoted from 22% (when re-suspended in pure water) to 98%. By a long-term observation (3-week), residual NaCl crystals on 0.9% saline treated copper surface were found partially disappeared in atmospheric environment, contributing to an additional Cu_2O layer forming above the treated surface. Besides, oxygen-containing species were observed even on fresh copper surface exposed by focused ion beam after saline treatment, suggesting a chloride-assisted atmospheric corrosion process.

Keywords: copper, cuprous oxide, chloride, corrosion, *E. coli*, antibacterial surface

1. Introduction

Antibacterial surfaces are drawing attentions in the recent years [1-3]. They can be applied as touched surfaces, having enormous potential demands in those heavily microbial burdened healthcare environments [4-6] as well as in our daily lives [7, 8]. In order to verify and assess the antibacterial ability of newly fabricated surfaces, antibacterial efficiency tests were designed and carried out.

Nowadays, there are different types of evaluation methods such as dry plating [9], wet plating [10], agar disk diffusion [11], etc. Limited by the incubation of bacteria and transfer process of bacterial suspension, a certain medium must be introduced during these evaluations. This medium is usually called buffer, which provides a suitable aqueous environment for bacterial survival without further growth. Despite the wide selection of buffers, in most of the cases, two main requirements should be satisfied: (1) a manageable pH range and (2) a suitable osmotic pressure for the microbes. Take phosphate-buffer saline (PBS) as an example [12], it contains a pair of acid and its conjugate base so as to compensate the pH fluctuation around 7.4. For the second purpose, it is sodium chloride (NaCl) that plays the part.

As can be seen, the design of buffers mainly considers the needs of microbes. But when they are to be applied in antibacterial surface research, a question needs to be raised: should the potential interactions between buffers and surfaces also be considered? The answer may be “certainly”. For example, copper-containing surfaces have been recently developed for antibacterial applications in various occasions [13-15]. Their antibacterial capability originates from the multifunctional antibacterial effects of copper ions [16]. To strongly interfere the survival of harmful microbes, copper ions should be efficiently released from the surfaces. As metallic surfaces, this release process is, most of the time, achieved by corrosion. The composition and the properties of buffer could become decisive, as they could facilitate or retard the corrosion process. Therefore, the solution and the copper surfaces together display how effective the antibacterial activity would be shown in antibacterial efficiency test.

Back to the example of PBS or other saline solutions, without a doubt, NaCl is expected to play an extremely important factor in revealing the antibacterial efficiency of copper surface. Electrochemical study has investigated the roles of chloride ions (Cl^-) in formation and transformation of corrosion product (CuCl, Cu_2O, $Cu(OH)_2$, etc.) [17], which could further affect the diffusion of copper ions [18]. In general, the presence of Cl^- also leads to a relatively corrosive environment for copper, depending on the concentration of Cl^- [19]. Meanwhile, it easily promotes pitting corrosion and further deterioration on the surface [20]. This could, on the contrary, contributes to the copper antibacterial efficiency. Because whenever the corrosion is enhanced, a faster dissolution process of the antibacterial substance (copper ions) is anticipated. For example, a latest study that evaluated antibacterial property of copper-silver surface has discovered the constructive effect of chloride addition in dissolving antibacterial copper ions [21]. Other experiments also suggest that Cu-Fenton chemistry, as one of the antibacterial mechanism, could be accelerated by Cl^- [22], resulting in a better biofilm removal. On the whole, a different

antibacterial efficiency is therefore highly expected in Cl^--containing environment.

Other than affecting the corrosion behaviour in media, it is noteworthy that NaCl deposits could induce atmospheric corrosion on dry surfaces. At high humidity levels, for instance, deliquescence of NaCl could happen, initiating micro-droplets formation on metallic surfaces and introducing further corrosion [23]. In lower humidity circumstances (below than 79% RH, deliquescence point of NaCl), where NaCl does not dissolve though, adsorption of water on the surface could form several layers that act as bulk water [24]. Diffusion of Cl^- could thus occur in this quasi-aqueous condition resulting in corrosion attack on copper [25]. Either way, tracking this atmospheric corrosion effect after antibacterial efficiency test may have significant implication for long-term product design [26].

Lately, we compared PBS and Na-4-(2-hydroxyethyl)-1-piperazineethanesulfonic acid (Na-HEPES) in terms of their impacts on evaluating the antibacterial performance of metallic copper and Cu_2O surface [27]. Corrosion behaviours introduced by PBS caught our attention, therefore further experiments were designed to reveal the roles of bacteria were revealed [28] and to discuss the corrosion attacks and oxide growth [29]. Since PBS contains NaCl, this study narrows down to it, to find out if NaCl plays an important factor as expected, in respect to corrosion. The primary objective is to explore how 0.9% saline affects the antibacterial efficiency test on metallic copper surface. Afterwards, the corrosion behaviours were compared among saline with different Cl^- or *Escherichia coli* (*E. coli*) concentrations. Finally, the following aging effects resulting from the residual NaCl crystals on copper surface were also characterised.

2. Materials and Methods

2.1. Materials

Copper (99.99%, K09, Wieland) coupons were ground with a silicon carbide sandpaper (stepped down to grit number P600), then cleaned with ethanol in an ultrasonic bath, finally dried by air.

2.2. Solutions

Saline with various final concentrations (0.45%, 0.9%, and 1.8%) was prepared with NaCl (VWR, Germany) and pure water for analysis (Merck, Germany), sterilised in an autoclave after preparation. PBS was prepared with NaH_2PO_4. $1H_2O$ (Merck, Germany, final concentration 0.01 M), NaCl (VWR, Germany, final concentration 0.14 M) and pure water for analysis, and its pH value was adjusted by adding NaOH to 7.4. Buffers were sterilised in an autoclave after preparation.

The preparation of bacterial suspension will be described in Section 2.6. Besides, a fivefold concentration *E. coli* NaCl suspension was simply prepared by re-suspending bacteria in 0.2 mL of NaCl instead of its original volume 1 mL. A tenth fold diluted *E. coli* NaCl suspension was prepared in the similar manner.

2.3. Corrosion protocol

Droplet of 20 µL pure solution or *E. coli* suspension was applied on ground copper surfaces with a pipette. These copper coupons were placed in a water-saturated atmosphere at room temperature for 3 h. Solutions or suspensions were then withdrawn with a pipette. These steps are chosen to simulate the antibacterial efficiency test further described in Section 2.6.

If not specified, the coupons were then cleaned with ethanol in an ultrasonic bath immediately after withdrawal of droplet. However, for the tests with various NaCl or bacterial concentrations (Section 3.4), the treated surfaces were firstly wiped with detergent-dipped cotton pads in order to remove the adhered bacteria. On the other hand, for some tests designed for atmospheric aging experiments (Section 3.5), the coupons remained unwashed. They were constantly kept in the lab atmosphere at room temperature, except for the time being characterised.

2.4. Surface characterization

Different functions of scanning electron microscope (SEM, Helios NanoLab600, FEI) were employed to observe copper surfaces after various corrosion experiments. Secondary electron detector (SE) was applied to examine the top-surface as well as cross-section of the coupons. Meanwhile, with backscatter electron detector (BSE), localised corrosion attacks covered by corrosion products were explored. Acceleration voltages will be further mentioned in the corresponding figure captions. The chemical composition of bacteria was obtained by Energy dispersive X-ray spectroscopy (EDS) at 5 kV. Optical microscope (OM, OLS4100, Olympus) photos were captured in 3D bright field mode. For further confirmation of the corrosion products covering the surfaces, high resolution grazing incidence X-ray diffractometer (GIXRD, Cu K_α with 1° grazing angle, PANalytical X'Pert PRO-MPD) was applied. In the atmospheric aging experiments, focused ion beam (FIB) was applied to fabricate fresh cross-section of the copper coupon after corrosion treatment, using gallium ions with an accelerating voltage of 30 kV. Images and spectra were obtained within 24 h after the corresponding corrosion treatments, except from the atmospheric aging experiments.

2.5. Copper content determination

After corresponding surface treatment, 10 µL samples were withdrawn by repetitive pipetting and diluted in 2.990 mL 1 wt% nitric acid (Merck, Germany). Before being measured by inductively coupled plasma mass spectrometry (ICP-MS, 7500cx, Agilent), 3 µL of 10 mg/L scandium and caesium internal standard solutions were added to the samples. For calibration, standards with 0.1, 0.5, 2.5, 10, 50, 250, and 1000 µg/L of copper were used. Original results with a unit of ppb were converted to the final values with µmol/L (µM), concerning both the fold of dilutions and molar mass 63.55 g/mol for copper. The average values and standard deviations were obtained by three independent experiments.

2.6. Antibacterial efficiency determination

Wet-plating test was used, whose details can be referred to a previous publication [10]. In brief, the *E. coli* K12 strain was grown aerobically overnight in Lysogeny broth (LB) medium at 37 ºC in a water bath with a speed of 220 rpm. The stationary cells from 1 mL culture were collected by centrifugation for 15 min at 5000×*g*, washed and centrifuged three times with the corresponding solutions, and finally re-suspended in 1 mL of the same type of solution. The test commenced by applying 20 µL of these re-suspended bacteria on the coupons, which were placed in a water-saturated atmosphere at room temperature. After 1 h, 10 µL samples were withdrawn by repetitive pipetting, serially diluted in PBS and spread on LB agar plates. Following incubation at 37 ºC for 24 h, the colony-forming unit (cfu) on agar plates was counted and expressed in a way concerning both the fold of dilutions and relative to the original 20 µL samples. The average values and standard deviations were obtained by three independent experiments.

3. Results and Discussion

3.1. Corrosion of copper surface in 0.9% NaCl and pure water

Before analysis of the actual antibacterial efficiency test, this study first focuses on the corrosive effects introduced by 0.9% NaCl (this concentration is hereafter simply referred to as "saline") without bacteria. For instance, Figure 1 (a-c) shows the morphological change and formation of corrosion product on the copper surface after 3 h exposure to this environment. Uniformly distributed sub-micron corrosion products are evident in SE image. Meanwhile, at some locations, much lower intensity was recorded in BSE (therefore darker), indicating missing of material underneath the corrosion product. These cavities signify where localised deterioration took place. Variation of microstructure definitely has impacts on the initiation of these localised attacks [30]. The distribution of these attacks can be mostly referred to a recent study [29], where how electropolished copper surface corroded by PBS droplet was investigated in detail.

Coupon exposed to pure water for the same duration is shown for comparison purposes in Figure 1 (d and e). Fewer features can be summarised: no obvious additional product coverage nor localised corrosion sites. Therefore, it can be preliminarily concluded that, adding NaCl into pure water significantly varies the environmental corrosivity towards copper.

The corrosion product formed on copper was further examined by high resolution GIXRD shown in Figure 1 (f). Crystalline Cu_2O has been identified as the major product after saline treatment, but not in pure water. Similar observation was obtained from potentiostatic polarisation [20], highlighting the formation of intermediate product CuCl, followed by the formation of Cu_2O and initiation of pits in a chronological sequence. However, CuCl is not identified in the current study. Meanwhile, the cavities were found being gradually covered by Cu_2O films, instead of destroying the films. Therefore, dissolution-precipitation or re-deposition mechanism [27] seems to be more appropriate in explaining the oxide growth: it is exceeding amount of copper ions gathering near the copper surface and forming oxide.

3.2. Corrosion of copper surface in bacterial suspensions

By adding *E. coli* (hereafter referred to as "bacteria"), solution becomes suspension, some corrosion behaviours on copper surface thus alter accordingly, as can be found in Figure 2. In saline, localised corrosion attack is still predominant, which can be easily recognised from the BSE images. SE image usually shows more morphological details, but the above-mentioned (Section 3.1) sub-micron corrosion product Cu_2O forming in pure solution can hardly be seen. The missing diffraction peak of Cu_2O (111) in GIXRD also matches this observation. Highly similar phenomena were recently reported in the case of PBS [28], which could help interpret the current scenario: it is attributed to the bacterial accumulation effects of copper ions. Copper concentration near surface is thus reduced and oxide growth is inhibited.

Without oxide coverage, a considerable amount of cavities, as a result of localised corrosion attacks, become visible even in SE mode. Those invisible ones, on the other hand, may imply another mechanism of pit initiation: a Cu_2O membrane could be found, separating the inner pitting region from the aqueous environment and promoting further pitting corrosion under the uppermost copper surface [31]. Similar sites have also been observed in the intermetallic particles induced crystallographic pitting grown beneath the surface [32], suggesting galvanic couple could be considered in the current scenario.

In the case of pure water, its bacterial suspension has not introduced distinct morphological or chemical changes on copper surface. These contrasts suggest the important roles of *E. coli*: although its presence inhibits the formation of Cu_2O, it does not affect the major corrosion attacks (especially in saline) or cause additional corrosion effect (especially in pure water). In other words, it is still the properties of solution that determine the corrosion process.

From the microbiological perspective, addition of bacteria introduces not only bacteria themselves, but also their metabolism as well as the products of it. Bacterial respiration, for example, is one of the universal processes frequently discussed, as it could help reducing oxygen content in the aqueous environment [33]. Meanwhile, dissolved oxygen happens to play an indispensable factor in the corrosion of metallic copper in aqueous [34] or Cl^--containing environment [35]. However, in the following sections, this aspect will be further ruled out from the present conditions.

3.3. Copper release and antibacterial efficiency

In the above sections, the corrosion behaviours of copper surface were revealed, in terms of how it varies after being exposed to different solutions or suspensions. But apart from this, it is also meaningful to investigate the effects of corrosion on the contacting droplet itself. For instance, the rise of copper content measured by ICP-MS shown in Figure 3 (a) offers valuable information. First of all, it is evident that the copper content measured from the bacterial suspension is higher than its corresponding pure solution. This can be again correlated with the role of bacterial addition summarised above: since bacteria decrease the amount of free copper ions in solutions, it favours a continuous release kinetics. This particularly

affects the situation in saline, as it suppresses the formation of Cu_2O, which could have formed as a barrier layer reducing the metal/solution interface [27] as well as retarding ion diffusion [18].

Another marked discrepancy is found between saline and pure water: the amounts of copper presented in saline are, in both cases, evidently higher than that in pure water. This trend matches the SEM observation: copper surface always suffers from more detectable localised corrosion attacks in saline. This is likely attributed to Cl^-, which has been regarded as an accelerator of corrosion on metallic surfaces most of the time [36]. With respect to copper, there was also study conducted on the relationship between Cl^- concentration and corrosion rate [19]. It shows that the Cl^- attachment allows complex formation and thereby promotes a faster ion release.

Additionally, it is still worth noting that neglectable variations of surface topography does not necessarily represent similar copper release level. In the case of pure water, although SEM results do not indicate significant difference, its bacterial suspension does enhance copper release by about three times, from 75.29 μM to 299.15 μM (data listed in the table in Figure 3). This suggests that it is the uniform corrosion that dominates the copper release in pure water, instead of localised corrosion.

Copper content presented in suspension is also positively related to the surface antibacterial efficiency, as presented in Figure 3 (b). Bacteria in both suspensions were grown from the same broths and thence share similar original concentration. Merely in 1 h, their survival already parted ways: around 98% were killed in the saline suspension, while only 22% was recorded in pure water. Not surprisingly, these numbers match the difference of copper content evaluated in ICP-MS shown above and that accumulated in the bacterium compared in Figure 3 (c): Stronger Cu L_α radiation at 0.930 keV was recorded from the bacteria in saline.

These comparisons demonstrate how corrosion behaviour and antibacterial efficiency are correlated: even though same type of microbe was tested on same type of metallic copper surface, the composition of the solution can dictate the release of antibacterial substance and thus result in a different antibacterial efficiency. Saline, a relatively corrosive solution, causes a higher amount of copper release (at least within a certain period), raising the copper concentration and enabling a faster killing rate against *E. coli*. A recent study [21] conducted by another research group also found out a similar role of Cl^- in enabling sufficient corrosion on not only copper and but also copper-silver alloy to deactivate *S. aureus*.

Two additional remarks may help further interpreting the antibacterial efficiency results. Since the killing rate follows the same trend of the increasing copper content, it cannot be estimated in the current experiment, how much of the antibacterial efficiency was assisted by the Cl^- accelerated Cu-Fenton reaction [22] or other combined effects [37]. On the other hand, one may notice that pure water is not a buffer, but a low osmolarity environment in the strict sense. Hypoosmotic shock does not necessarily lead to cell death [38], but even if it does, the contribution of copper in reaching a 22% killing rate should be considered even lower.

3.4. Effects of NaCl concentration and *E. coli* concentration on copper

Since the effects of NaCl and *E. coli* in this corrosion system have been preliminarily identified, additional experiments were designed to explore these effects. Figure 4 (a-c) compare the effects of saline concentration on the corrosion behaviours of copper surface. For all these selected concentrations, copper was subjected to a similar type of localised corrosion attacks. As the saline concentration increases, the expansion of cavities is observed, identified by imaging contrast in BSE. Besides, contrast can also be found even within a single cavity. This implies the localised attack inside the cavity is not uniform. On the other hand, oxide growth is ignorable in both 0.45% and 0.9% suspensions. But when it added up to 1.8%, huge areas covered by sub-micron oxides are found. Meantime another striking feature is also observed regarding the distribution of oxide on copper surface: they only grew on specific locations.

According to the re-deposition mechanism discussed (at the end of Section 3.1), oxide growth usually corresponds to excessive copper ions. Therefore, the emergence of oxide could be attributed to a faster corrosion kinetics in a high Cl^- concentration scenario, where the amount of copper ions exceeds the accumulation capacity of *E. coli*. However, as the bacteria presenting in the droplet are supposed to be well-mixed, their copper accumulation effect should be distributed evenly on the surface. That is to say, the localised copper ion concentration is expected similar across the whole near surface. Therefore, other than copper concentration, there must be another factor governing the preferential locations of oxide growth.

As it can be seen in Figure 4 (d), oxide coverage seems to follow the grinding marks. It strongly suggests its correlation with the state of the original copper surface (*e.g.* microstructural or morphological difference introduced by the grinding procedure). In other words, variation of the state of the surface might dominate the distribution of cathodic sites, where oxide growth prevails. To design similar experiments on electropolished copper surface may help, as it did reveal the crystallographic tendency of copper corrosion in PBS [29].

To verify the role of ion accumulation effect introduced by *E. coli*, another corrosion test was conducted with 1.8% NaCl, whereas fivefold *E. coli* was re-suspended. After the same duration, oxide coverage can hardly be seen on copper surface, as shown in Figure 5 (a). Surge of the amount of bacteria boosts both the capacity and efficiency of the ion accumulation, compensating the increase of copper release in high Cl^- concentration. Besides, higher bacterial concentration did not affect the selective distribution of localised corrosion sites, indicating that the corrosion mechanism stays the same. However, the size of cavities did shrink, and easy to be found connected altogether. Meanwhile, even on the locations that are free from severe localised corrosion, slight degradation can be observed, as the grinding marks can hardly be found. It is unclear at the current stage, but these phenomena could be related to but not limited to the variation of local chemical concentration (Cl^- or chemicals produced by bacterial metabolism), local fluid flow rate (induced by the mobility of bacteria), etc.

On the other hand, with lower bacterial concentration (tenth fold diluted), oxide coverage can always be found in

whole series of NaCl concentration (Figure 5 (b-d)). Oxide particles with bigger size are noticed in lower NaCl concentration. That is, NaCl concentration has an impact on the nucleation density of oxide. The trend of how NaCl and bacterial concentration influence oxide growth and corrosion attacks are qualitatively summarised in Figure 5 (e).

3.5. Atmospheric corrosion caused by residual NaCl crystals

So far, the impacts of NaCl on copper surface have only been discussed during corrosion test or antibacterial efficiency test. However, even though the saline will be withdrawn afterwards, some NaCl residues could stay on the copper surface. These NaCl crystals are found to continue playing a decisive part in the copper aging process.

Figure 6 compares the copper surfaces observed 3 weeks after having been exposed to saline. Coupon shown in Figure 6 (a) has been cleaned immediately after the saline was withdrawn in the end of the corrosion test, therefore no NaCl crystal was remained. In this case, the oxide coverage is found unchanged in 3 weeks. However, coupon that has not been cleaned properly experienced significant changes, as shown in Figure 6 (b). Firstly, a secondary layer with a slightly different roughness formed on the previous Cu_2O coverage. Moreover, the reason why some uncovered previous Cu_2O can be located, is likely related to the NaCl crystals (with brighter colour in SE mode) lying aside: it is assumed that these uncovered zones were also originally covered by the NaCl crystals. Nevertheless, these crystals gradually disappeared during the 3-week atmospheric aging.

From GIXRD results, two facts have been clearly shown. First, NaCl residues were efficiently cleaned by the current protocol, as much weak diffraction signals are found on the cleaned coupon. Second, more Cu_2O diffraction peaks with higher intensity appeared from the coupon without cleaning, confirming the newly grown secondary layer is mainly composed of Cu_2O as well.

Intriguingly, this kind of aging effect does not occur only on the directly treated copper surface. As shown in Figure 7, a hole on the copper coupon was fabricated by FIB, immediately after the corrosion test without applying cleaning protocol. This exposes some “fresh” areas beneath the original surface. “Fresh” is here defined as having not directly “met” the saline, since they were still inside the bulk copper during the corrosion test. OM image taken straightway after FIB operation (*i.e.* Day 0) recorded some bright zones, not just in the hole, but also around it, as a result of Ga ion beam bombardment. The areas inside the hole that are darker were due to rougher topography, confirmed by SEM images.

However, as the aging experiment proceeds, the bright zones shown in OM turned darker from the boundaries inwardly. This is related to the morphological changes displayed in Figure 8: submicron particles were forming on top of these surfaces. Being continuously exposed to atmosphere, part of this region extended, from the cross-section (edge of the hole) towards the bottom of it. Meanwhile, coarsening can be observed on some of these particles. At the cross-section (invisible in OM owing to observation angle) which is supposed to be relatively smooth at the original state, similar particle formation and coarsening phenomenon are also found. Although the exact chemical or phase composition has yet to be determined,

these locations do contain an extra amount of oxygen content (Figure 8 (d&e), obvious O K_α radiation at 0.525 keV), suggesting the formation oxygen-containing species. Served as the control groups, same type of FIB cross-sections was produced on copper coupon exposed to either pure water or *E. coli* water suspension for the same duration. Neither of these surfaces shows such changes after 3 weeks (data not included), excluding the potential additional effects brought by Ga ion implantation during FIB operation.

All these comparisons help to preliminarily pin down the cause of atmospheric aging: NaCl, as it the only varied environmental parameter. As the solution cannot been withdrawn completely, NaCl crystallised locally on the copper surface after the remained water evaporated. However, this is not yet the final fate of these crystals. Atmospheric corrosion continues to play a role. For example, these salts could go through a process so-called deliquescence [23], thereby absorbs the water from the atmosphere and induce aqueous corrosion. But this process requires a relatively high humidity (79% RH for pure NaCl), which is usually not fulfilled in the lab environment.

In spite of this, NaCl crystals could transform in another way, which is still related to water absorption, not by NaCl itself, but by the general surface. Because it is common to find monolayers of water forming on surfaces [24]. Therefore, the copper surface could still be regarded as being exposed to a quasi-aqueous environment. In fact, the properties of the water layer could already affect the nucleation and formation rate of Cu_2O in a certain range of relative humidity [39]. Besides, these monolayers dissolve NaCl and transform itself to electrolyte. Meanwhile, Cl^- are able to diffuse through these monolayers, reaching to the other parts of the surface [25]. Considering this circumstance, corrosion related phenomena are not a surprise. In addition, Cl^- may not be the only ions that would diffuse through the surface, as copper ions should also participate a similar process. Take the saline corroded surface as an example (Figure 6 (b)), without copper ion diffusion to the top of the existing Cu_2O, it is hard to imagine how the secondary layer of Cu_2O actually formed on top.

3.6. Insight into antibacterial surface research

Firstly, the current results suggest the significance of buffer selection in antibacterial surface research. Buffers are more than a friendly environment designed for microbes. On the contrary, depending on their components as well as the corresponding properties (corrosivity in this case), they may react with the investigated surface in different ways, resulting in an enhanced antibacterial efficiency or vice versa. Evidences for this can also be obtained from other comparisons such as PBS vs Na-HEPES [27], or nutrient broth (NB) vs minimal media (MM) [40]. For the same reason, design of materials with weaker corrosion resistance could enhance release of antibacterial substances [41], meanwhile considering that the cytotoxicity might need to be and definitely can be avoided in specific scenarios [42].

Secondly, growth and coverage of passive layer as a result of the subsequent atmospheric corrosion, may not be beneficial for the long-term antibacterial property of antibacterial copper surface [26]. Therefore, it should particularly inspire the applied research closely related to touched surfaces, as NaCl is also one of the major residues of perspiration. To

evaluate its effect on antibacterial efficiency, cyclic test [43] should be one of the effective ways to be included in the future work.

4. Conclusion

NaCl as a common component in many popular buffers, was examined in this work in view of its roles in copper corrosion. Some concluding remarks are summarised as below:

- Ground copper coupon undergoes severe localised corrosion attacks in the environment of 0.9% saline, regardless of whether *E. coli* is added or not.
- A layer of Cu_2O grows on copper surface when being exposed to pure 0.9% saline. In the case of its *E. coli* suspension, formation of Cu_2O has been inhibited at least in 3 h.
- A faster killing rate of ground copper surface against *E. coli* (98% in 1 h) is recorded in 0.9% saline, compared to pure water (22%), which is attributed to the accelerated corrosion process in the presence of Cl^-.
- Increase of Cl^- concentration may accelerate copper release, forming Cu_2O even in *E. coli* suspension. However, it can be counteracted by increasing the concentration of *E. coli* to fivefold, as this enhances the copper ion accumulation effect.
- Residual NaCl crystals on copper surface promote the formation of additional Cu_2O as corrosion products. A Cl^--assisted atmospheric corrosion process is revealed by a FIB-assisted 3-week aging experiment.

Acknowledgements

This study was supported by Erasmus Mundus Joint European Doctoral Programme in Advanced Materials Science and Engineering (DocMASE, 512225-1-2010-1-DE-EMJD, European Commission) and the PhD-Track-Programme (PhD02-14, Franco-German University). The ICP-MS experiments were supported by Dr. Ralf Kautenburger from the chair of Inorganic Solid State Chemistry. J. L. particularly thank Prof. Tomáš Prošek from University of Chemistry and Technology Prague, for his inspiring perspective during EUROCORR 2018 and 2019, making this work possible.

Declarations of interest

None.

Data availability

The data that support the findings of this study are available from the corresponding author on request.

References

[1] M. Vincent, R.E. Duval, P. Hartemann, M. Engels‐Deutsch, Contact killing and antimicrobial properties of copper, Journal of Applied Microbiology, 124 (2018) 1032-1046.

[2] S. Rigo, C. Cai, G. Gunkel-Grabole, L. Maurizi, X. Zhang, J. Xu, C.G. Palivan, Nanoscience-Based Strategies to Engineer Antimicrobial Surfaces, Advanced Science, 5 (2018) 1700892.

[3] M.P. Muller, C. MacDougall, M. Lim, I. Armstrong, A. Bialachowski, S. Callery, W. Ciccotelli, M. Cividino, J. Dennis, S. Hota, G. Garber, J. Johnstone, K. Katz, A. McGeer, V. Nankoosingh, C. Richard, M. Vearncombe, Antimicrobial surfaces to prevent healthcare-associated infections: a systematic review, Journal of Hospital Infection, 92 (2018) 7-13.

[4] S.S. Dunne, M. Ahonen, M. Modic, F.R.L. Crijns, M.M. Keinänen-Toivola, R. Meinke, C.W. Keevil, J. Gray, N.H. O'Connell, C.P. Dunne, Specialised cleaning associated with antimicrobial coatings for reduction of hospital acquired infection. Opinion of the COST Action Network AMiCI (CA15114), Journal of Hospital Infection, (2018).

[5] M. Colin, F. Klingelschmitt, E. Charpentier, J. Josse, L. Kanagaratnam, C. De Champs, S.C. Gangloff, Copper Alloy Touch Surfaces in Healthcare Facilities: An Effective Solution to Prevent Bacterial Spreading, Materials, 11 (2018) 2479.

[6] S. Chyderiotis, C. Legeay, D. Verjat-Trannoy, F. Le Gallou, P. Astagneau, D. Lepelletier, New insights on antimicrobial efficacy of copper surfaces in the healthcare environment: a systematic review, Clinical Microbiology and Infection, (2018).

[7] J.H. Michel, W.R. Moran, A.A. Estelle, K.E. Sexton, H.T. Michels, Antimicrobial Benefits of Copper Alloy Touch Surfaces, Int. J. Powder Metall., 49 (2013) 33-36.

[8] G. Grass, C. Rensing, M. Solioz, Metallic Copper as an Antimicrobial Surface, Applied and Environmental Microbiology, 77 (2011) 1541-1547.

[9] S.L. Warnes, C.W. Keevil, Mechanism of Copper Surface Toxicity in Vancomycin-Resistant Enterococci following Wet or Dry Surface Contact, Applied and Environmental Microbiology, 77 (2011) 6049-6059.

[10] C. Molteni, H.K. Abicht, M. Solioz, Killing of Bacteria by Copper Surfaces Involves Dissolved Copper, Applied and Environmental Microbiology, 76 (2010) 4099-4101.

[11] S. Sonia, R. Jayasudha, N.D. Jayram, P.S. Kumar, D. Mangalaraj, S.R. Prabagaran, Synthesis of hierarchical CuO nanostructures: Biocompatible antibacterial agents for Gram-positive and Gram-negative bacteria, Current Applied Physics, 16 (2016) 914-921.

[12] Phosphate-buffered saline (PBS), Cold Spring Harbor Protocols, 2006 (2006) pdb.rec8247.

[13] Y. Sun, V. Tran, D. Zhang, W.B. Wang, S. Yang, Technology and Antimicrobial Properties of Cu/TiB2 Composite Coating on 304 Steel Surface Prepared by Laser Cladding, Materials Science Forum, 944 (2019) 473-479.

[14] K. Steinhauer, S. Meyer, J. Pfannebecker, K. Teckemeyer, K. Ockenfeld, K. Weber, B. Becker, Antimicrobial efficacy and compatibility of solid copper alloys with chemical disinfectants, PLoS ONE, 13 (2018) e0200748.

[15] C. Hahn, M. Hans, C. Hein, A. Dennstedt, F. Mücklich, P. Rettberg, C.E. Hellweg, L.I. Leichert, C. Rensing, R. Moeller, Antimicrobial properties of ternary eutectic aluminum alloys, BioMetals, 31 (2018) 759-770.
[16] M. Solioz, Copper and Bacteria: Evolution, Homeostasis and Toxicity, Springer, 2018.
[17] C. Toparli, S.W. Hieke, A. Altin, O. Kasian, C. Scheu, A. Erbe, State of the Surface of Antibacterial Copper in Phosphate Buffered Saline, Journal of The Electrochemical Society, 164 (2017) H734-H742.
[18] B.J. Webster, S.E. Werner, D.B. Wells, P.J. Bremer, Microbiologically Influenced Corrosion of Copper in Potable Water Systems—pH Effects, Corrosion, 56 (2000) 942-950.
[19] S.M. Mayanna, T.H.V. Setty, Role of chloride ions in relation to copper corrosion and inhibition, Proceedings of the Indian Academy of Sciences - Section A, 80 (1974) 184-193.
[20] A. El Warraky, H.A. El Shayeb, E.M. Sherif, Pitting corrosion of copper in chloride solutions, Anti-Corrosion Methods and Materials, 51 (2004) 52-61.
[21] N. Ciacotich, M. Kilstrup, P. Møller, L. Gram, Influence of chlorides and phosphates on the antiadhesive, antibacterial, and electrochemical properties of an electroplated copper-silver alloy, Biointerphases, 14 (2019) 021005.
[22] L. Wang, Y. Miao, M. Lu, Z. Shan, S. Lu, J. Hou, Q. Yang, X. Liang, T. Zhou, D. Curry, K. Oakes, X. Zhang, Chloride-accelerated Cu-Fenton chemistry for biofilm removal, Chemical Communications, 53 (2017) 5862-5865.
[23] S.X. Li, L.H. Hihara, Atmospheric corrosion initiation on steel from predeposited NaCl salt particles in high humidity atmospheres, Corrosion Engineering, Science and Technology, 45 (2010) 49-56.
[24] E. Schindelholz, R.G. Kelly, Wetting phenomena and time of wetness in atmospheric corrosion: a review, Corrosion Reviews, 30 (2012).
[25] Z.Y. Chen, S. Zakipour, D. Persson, C. Leygraf, Effect of Sodium Chloride Particles on the Atmospheric Corrosion of Pure Copper, Corrosion, 60 (2004) 479-491.
[26] M.J. Hutchison, J.R. Scully, Solute Capture and Doping of Al in Cu2O: Corrosion, Tarnish Resistance, and Cation Release of High-Purity Cu-Al Alloys in Artificial Perspiration, Journal of The Electrochemical Society, 165 (2018) C689-C702.
[27] J. Luo, C. Hein, J.-F. Pierson, F. Mücklich, Early-stage corrosion, ion release, and the antibacterial effect of copper and cuprous oxide in physiological buffers: Phosphate-buffered saline vs Na-4-(2-hydroxyethyl)-1-piperazineethanesulfonic acid, Biointerphases, 14 (2019) 061004.
[28] J. Luo, C. Hein, J. Ghanbaja, J.-F. Pierson, F. Mücklich, Bacteria accumulate copper ions and inhibit oxide formation on copper surface during antibacterial efficiency test, Micron, 127 (2019) 102759.
[29] J. Luo, C. Hein, J.-F. Pierson, F. Mücklich, Localised corrosion attacks and oxide growth on copper in phosphate-buffered saline, Materials Characterization, 158 (2019) 109985.
[30] A. Vinogradov, T. Mimaki, S. Hashimoto, R. Valiev, On the corrosion behaviour of ultra-fine grain copper, Scripta Materialia, 41 (1999) 319-326.

[31] C.A.C. Sequeira, Inorganic, physicochemical, and microbial aspects of copper corrosion: literature survey, British Corrosion Journal, 30 (1995) 137-153.
[32] H. Kakinuma, I. Muto, Y. Oya, Y. Kyo, Y. Sugawara, N. Hara, Mechanism for the Morphological Change from Trenching to Pitting around Intermetallic Particles in AA1050 Aluminum, Journal of The Electrochemical Society, 166 (2019) C19-C32.
[33] A.K. Lee, D.K. Newman, Microbial iron respiration: impacts on corrosion processes, Appl Microbiol Biotechnol, 62 (2003) 134-139.
[34] A. Hedin, A.J. Johansson, C. Lilja, M. Boman, P. Berastegui, R. Berger, M. Ottosson, Corrosion of copper in pure O2-free water?, Corrosion Science, 137 (2018) 1-12.
[35] W.D. Bjorndahl, K. Nobe, Copper Corrosion in Chloride Media. Effect of Oxygen, Corrosion, 40 (1984) 82-87.
[36] T. Prosek, A.L. Gac, D. Thierry, S.L. Manchet, C. Lojewski, A. Fanica, E. Johansson, C. Canderyd, F. Dupoiron, T. Snauwaert, F. Maas, B. Droesbeke, Low-Temperature Stress Corrosion Cracking of Austenitic and Duplex Stainless Steels Under Chloride Deposits, Corrosion, 70 (2014) 1052-1063.
[37] J.M. Cassells, M.T. Yahya, C.P. Gerba, J.B. Rose, Efficacy of a combined system of copper and silver and free chlorine for inactivation of Naegleria fowleri amoebas in water, Water Science and Technology, 31 (1995) 119-122.
[38] I.R. Booth, P. Louis, Managing hypoosmotic stress: Aquaporins and medianosensitive channels in Escherichia coli, Current Opinion in Microbiology, 2 (1999) 166-169.
[39] T. Aastrup, M. Wadsak, M. Schreiner, C. Leygraf, Experimental in situ studies of copper exposed to humidified air, Corrosion Science, 42 (2000) 957-967.
[40] M.A. Javed, P.R. Stoddart, E.A. Palombo, S.L. McArthur, S.A. Wade, Inhibition or acceleration: Bacterial test media can determine the course of microbiologically influenced corrosion, Corrosion Science, 86 (2014) 149-158.
[41] S.C. Tao, J.L. Xu, L. Yuan, J.M. Luo, Y.F. Zheng, Microstructure, mechanical properties and antibacterial properties of the microwave sintered porous Ti–3Cu alloys, Journal of Alloys and Compounds, 812 (2020) 152142.
[42] L. Fowler, H. Engqvist, C. Öhman-Mägi, Effect of Copper Ion Concentration on Bacteria and Cells, Materials, 12 (2019) 3798.
[43] S. Rtimi, R. Sanjines, M. Bensimon, C. Pulgarin, J. Kiwi, Accelerated Escherichia coli inactivation in the dark on uniform copper flexible surfaces, Biointerphases, 9 (2014) 029012.

Figure Captions

Figure 1

Typical SEM images of ground copper surfaces after 3 h exposure to 0.9% NaCl **(a-c)** or pure water **(d, e)**. Images were obtained by SE detector **(a, d)** and BSE detector **(b, c, e)** at 20 kV. The dotted lines in **(a, b)** surround a typical localised corrosion zone. Images **(a, b)** correspond to the square dash marked region in **(c)**. High resolution GIXRD results **(f)** in the range of (111) planes of Cu_2O (JCPDS#75-1531) obtained from these surfaces.

Figure 2

Typical SEM images of ground copper surfaces after 3 h exposure to *E. coli* 0.9% NaCl suspension **(a-c)** or *E. coli* pure water suspension **(d, e)**. Images were obtained by SE detector **(a, d)** and BSE detector **(b, c, e)** at 20 kV. The dotted lines in **(a, b)** indicate two types of localised corrosion site. Images **(a, b)** correspond to the square dash marked region in **(c)**. High resolution GIXRD results **(f)** in the range of (111) planes of Cu_2O (JCPDS#75-1531) obtained from these surfaces.

Figure 3

Copper content **(a)** in 0.9% NaCl or pure water, with or without *E. coli* after 3 h exposed to ground copper surfaces. Antibacterial efficiency test **(b)** against *E. coli* in two different suspensions in 1 h. The error bars indicate the standard deviations calculated from three independent measurements. Percentages in **(b)** above the bars represent the killing rate in 1 h (compared to the original data). Average values from **(a)** and **(b)** are listed in the tables. Typical EDS results **(c)** collected from the bacterium (*E. coli*) transferred onto silicon wafer after being treated with copper surface in two suspension for 3 h.

Figure 4

Typical SEM images (BSE, 5 kV) of ground copper surfaces after 3 h exposure to *E. coli* suspension with different NaCl concentration: **(a)** 0.45%; **(b)** 0.9%; **(c)** 1.8%. The dotted lines in **(a, c)** indicate typical localised corrosion cavities. Image **(c)** corresponds to the square dash marked region in **(d)**. Orange arrows in **(d)** indicate regions with oxide growth, while white arrows for those without.

Figure 5

Typical SEM images (BSE, 5 kV) of ground copper surfaces after 3 h exposure to **(a)** fivefold *E. coli* 1.8% NaCl suspension; **(b)** tenth fold diluted *E. coli* 0.45% NaCl suspension; **(c)** tenth fold diluted *E. coli* 0.9% NaCl suspension; **(d)** tenth fold diluted *E. coli* 1.8% NaCl suspension. Dash line in **(a)** separates the severe corrosion zone from the almost intact zone. Table **(e)** summarises the characteristics of oxide growth and corrosion sites in different conditions: more "+" represents

463 bigger particle size; more "-" represents smaller localised corrosion sites; "X" represents situations where particle coverage
464 was rarely observed.
465
466 Figure 6
467 Typical SEM images (SE, 5 kV) of ground copper surfaces 3 weeks after 3 h exposure to 0.9% NaCl solution. Coupon
468 shown in **(a)** has been ultrasonic cleaned by ethanol immediately after the 3 h corrosion experiment, while **(b)** was kept
469 without further cleaning. Both images share the same scale bars that presented in **(a)**. The dotted region in **(b)** indicates the
470 missing of NaCl crystal as well as the exposed original oxidised copper surface. High resolution GIXRD results **(c)** obtained
471 from these surfaces 12 weeks after the original treatment. Cu (JCPDS#04-0836), NaCl (JCPDS#05-0628), and Cu_2O
472 (JCPDS#75-1531) were applied to index the patterns. The diffraction peaks marked with hexagonal star (✸) represent
473 diffraction of Cu (111) planes under Cu-K_β and W-$L_{\alpha 1}$.
474
475 Figure 7
476 OM images **(a-d)** and SEM images **(e-k)** (SE, 5 kV, coupon being 52° tilted) of fresh section of copper surface prepared by
477 FIB after 3 h exposure to 0.9% NaCl. OM images and SEM images share the same scale bars presented in **(a)** and **(e)**,
478 respectively. This position was repeatedly examined every 7 days. Dark areas surrounded by dotted lines in **(a)** are the
479 regions pointed out by arrows in **(e)**. Area marked with dotted line in **(d)** serves as an example for positions that suffered
480 colour change compared to the same positions in **(a)**. High magnification images of the square dash marked regions in **(f-h)**
481 are further shown in the following Figure 8. A schematic description of the treatment process is shown below the graphs.
482
483 Figure 8
484 High resolution SEM images **(a-c)** (SE, 5 kV, coupon being 52° tilted) of fresh section of copper surface prepared by FIB
485 after 3 h exposure to 0.9% NaCl solution. This position was repeatedly examined every 7 days **(a-c)**, whose lower
486 magnification images are already presented in Figure 7. Zone covered by light blue colour in **(a)** highlights the cross-section
487 (edge of the hole). Image **(d)** (SE, 5 kV) was taken from the Day 21 coupon. The cross shape indicator points out the
488 position where the EDS spectrum **(e)** was collected.

Figure 1

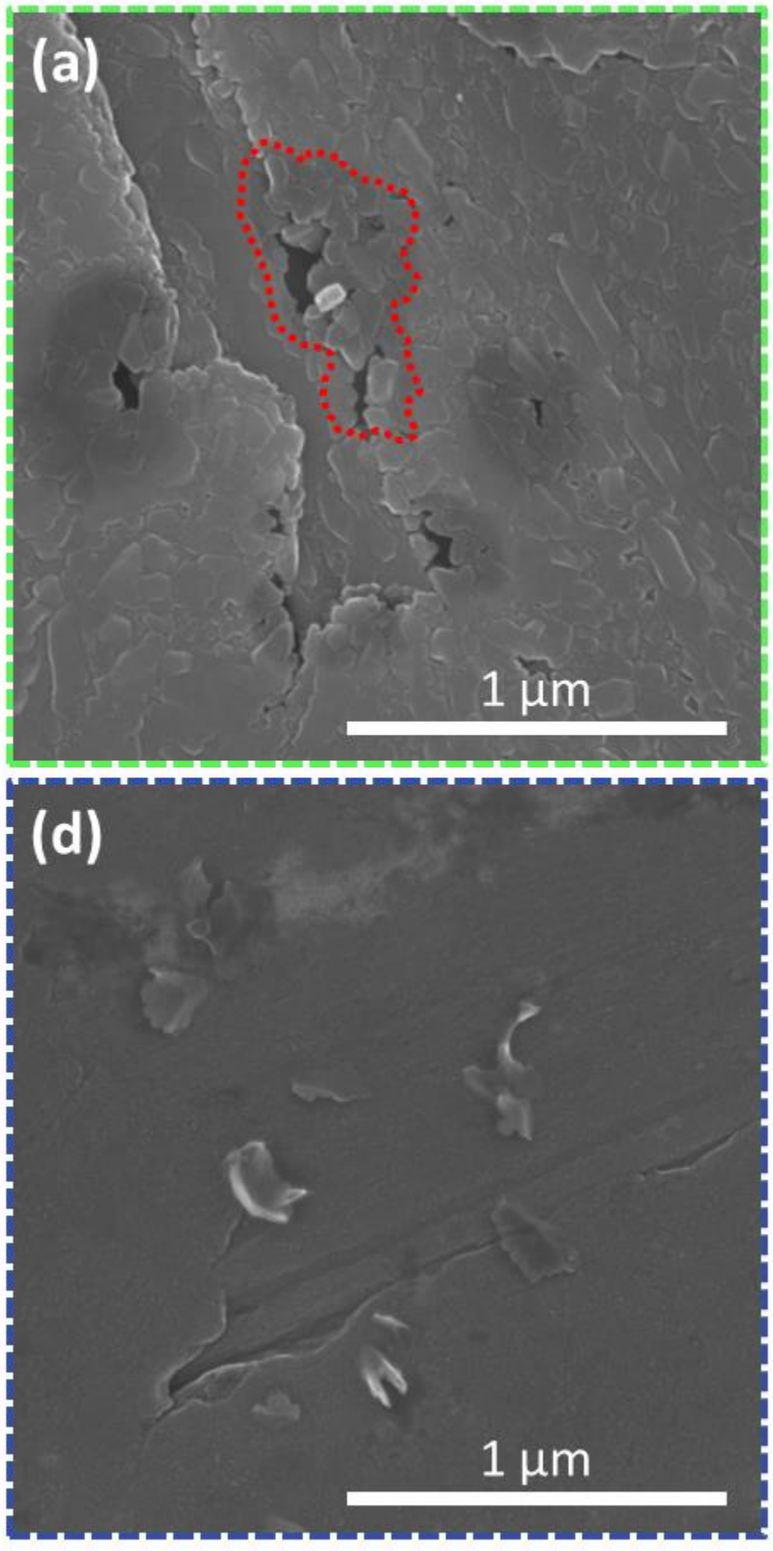
(a)
1 µm

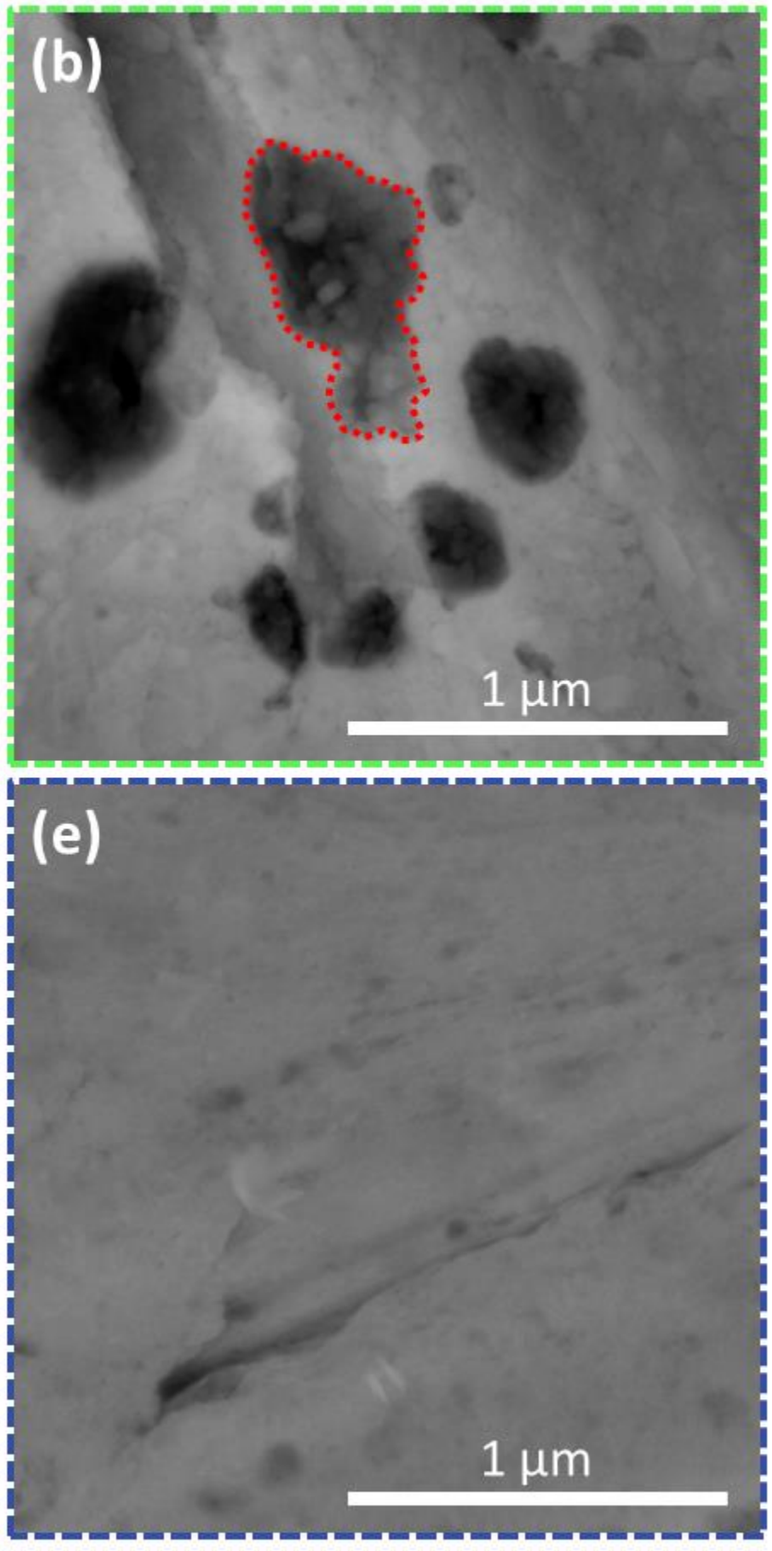
(b)
1 µm

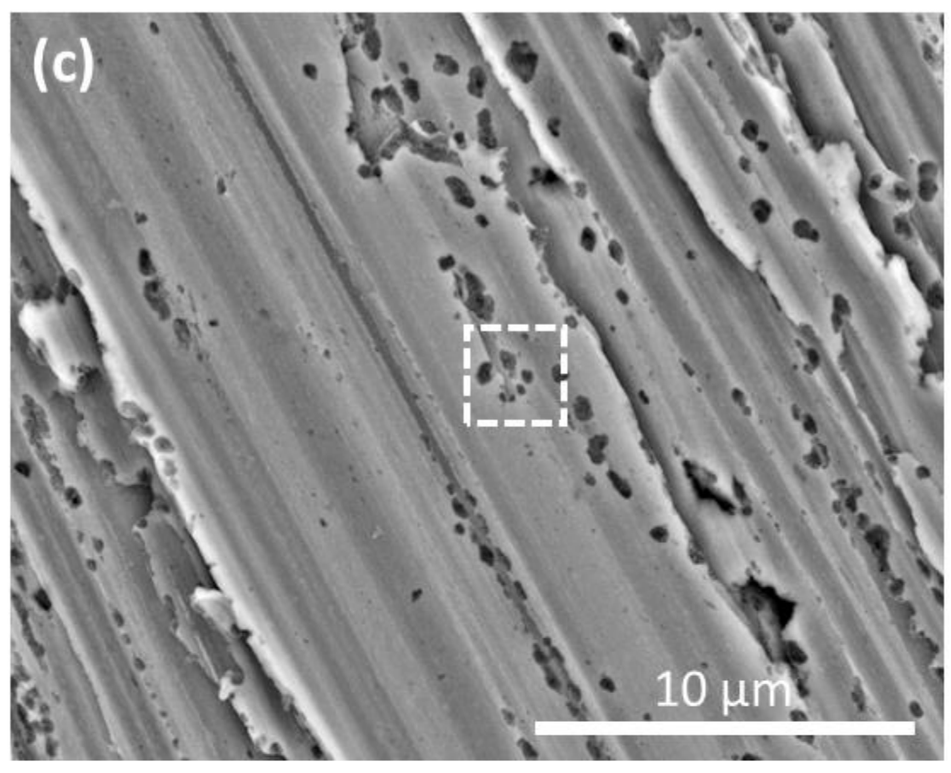
(c)
10 µm

(d)
1 µm

(e)
1 µm

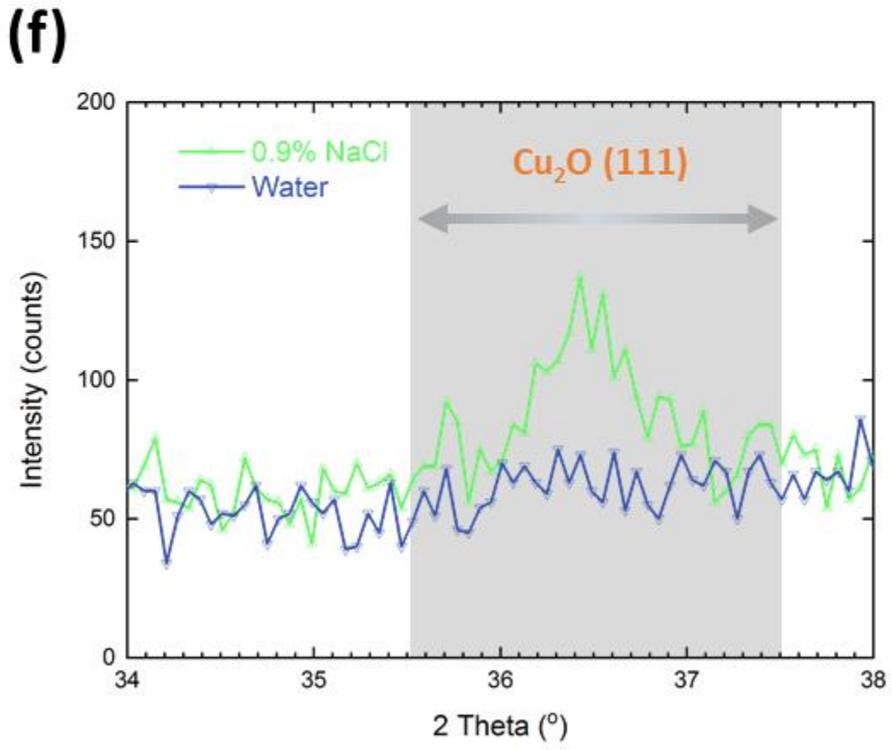
(f)
0.9% NaCl
Water
Cu2O (111)
Intensity (counts)
2 Theta (°)
0
50
100
150
200
34
35
36
37
38

Figure 2

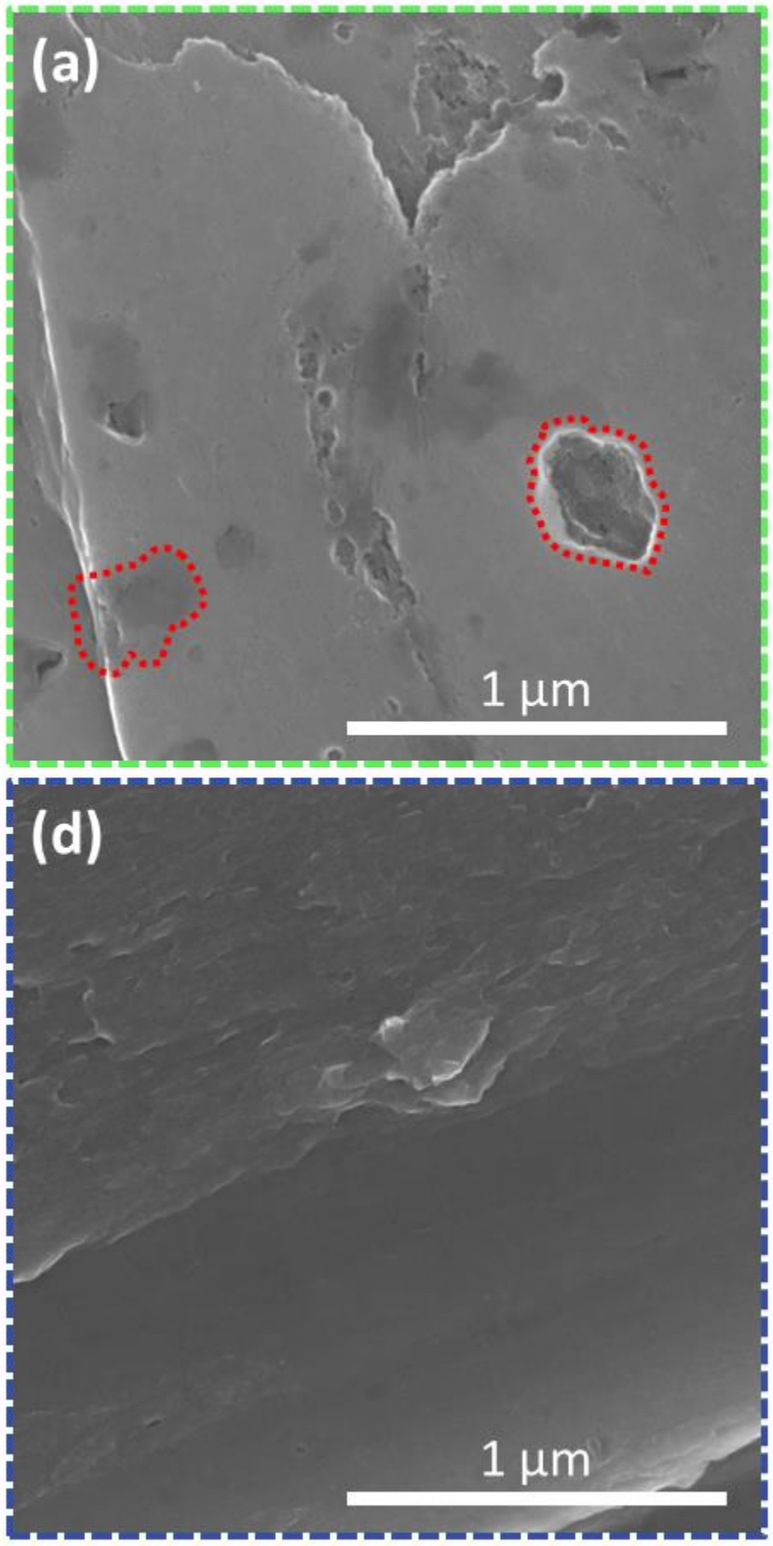
(a)
1 µm

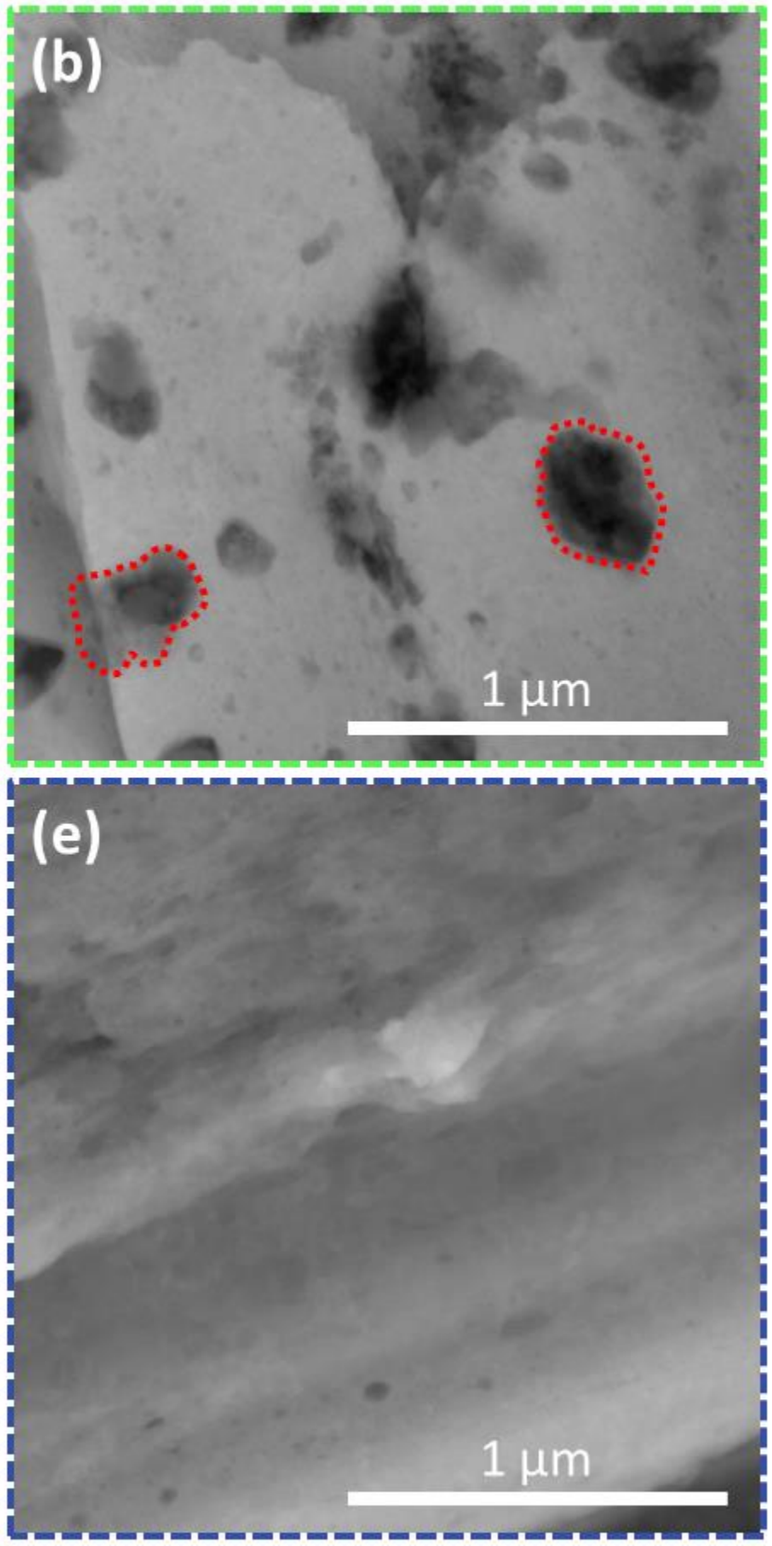
(b)
1 µm

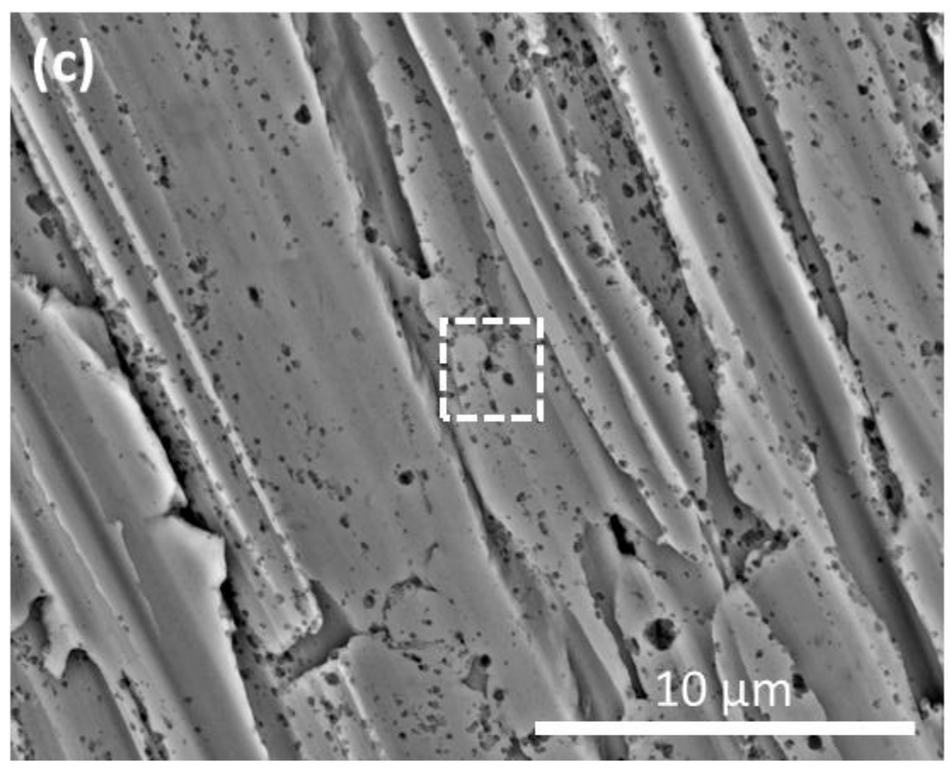
(c)
10 µm

(d)
1 µm

(e)
1 µm

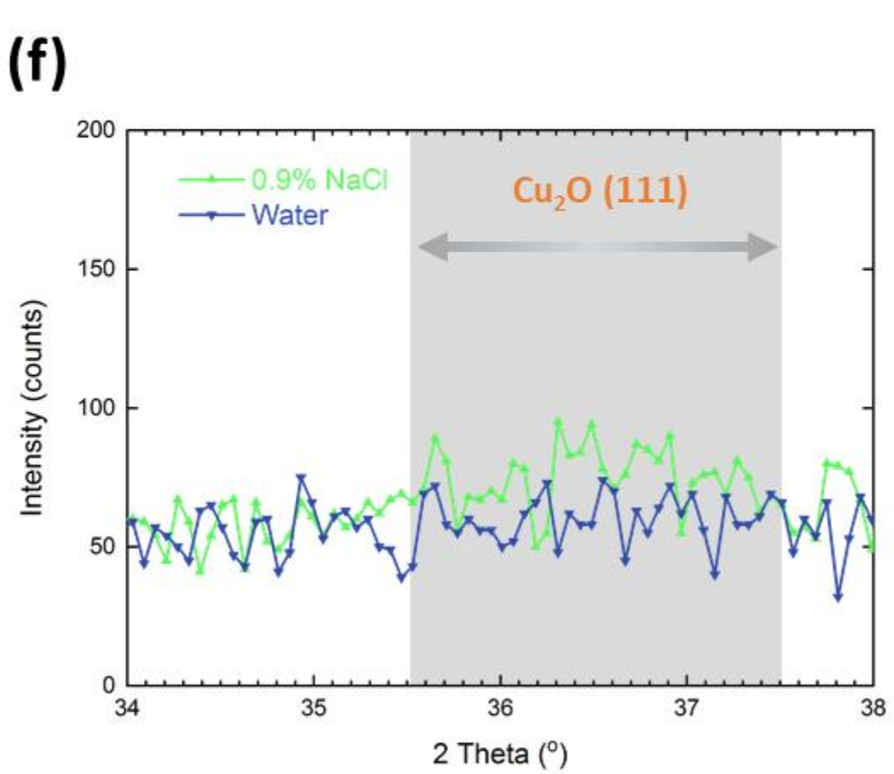
(f)
0.9% NaCl
Water
Cu2O (111)
Intensity (counts)
2 Theta (°)
0
50
100
150
200
34
35
36
37
38

Figure 3

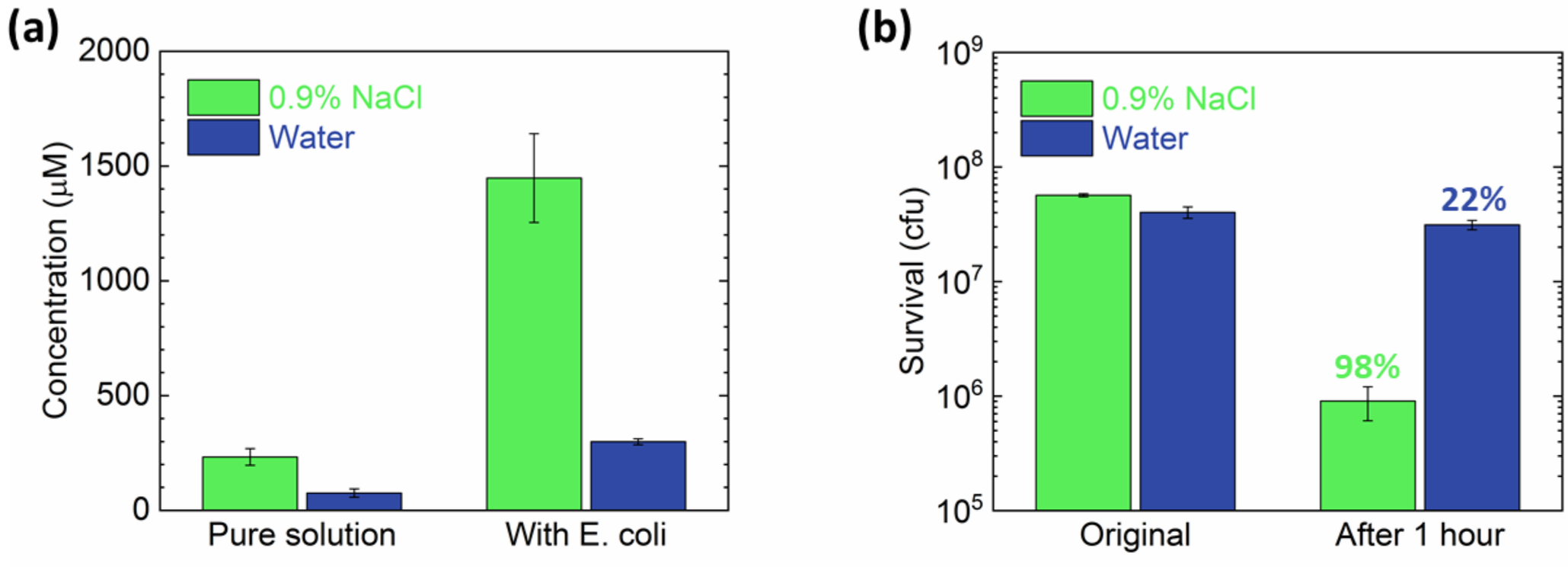

Copper concentration (μM)

Pure solution		With *E. coli*	
0.9% NaCl	Water	0.9% NaCl	Water
232.64	75.29	1447.60	299.15

Survival (cfu)

Original		After 1 hour	
0.9% NaCl	Water	0.9% NaCl	Water
5.66E+07	4.01E+07	9.07E+05	3.12E+07

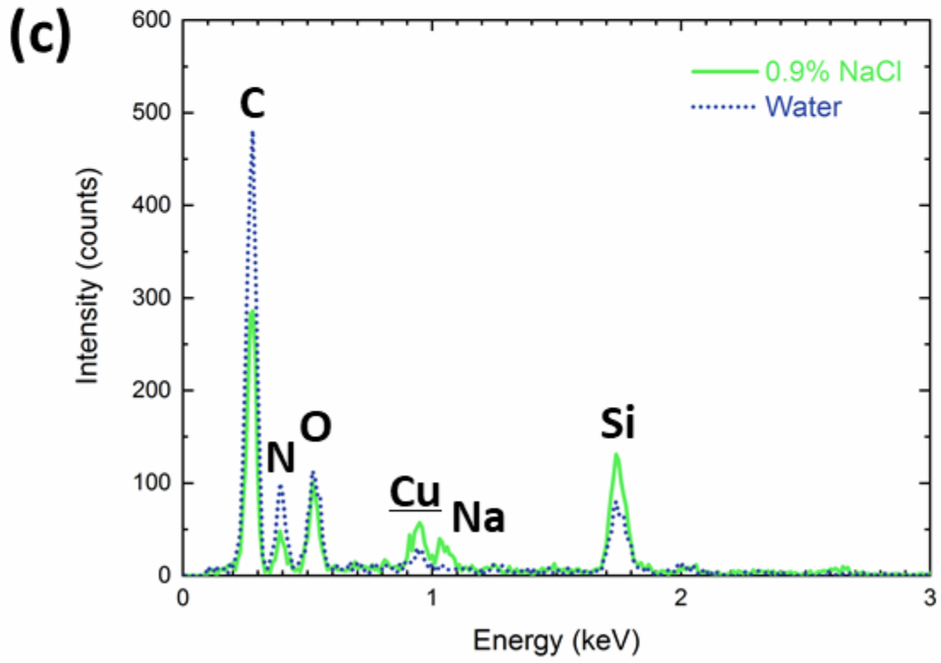

Figure 4

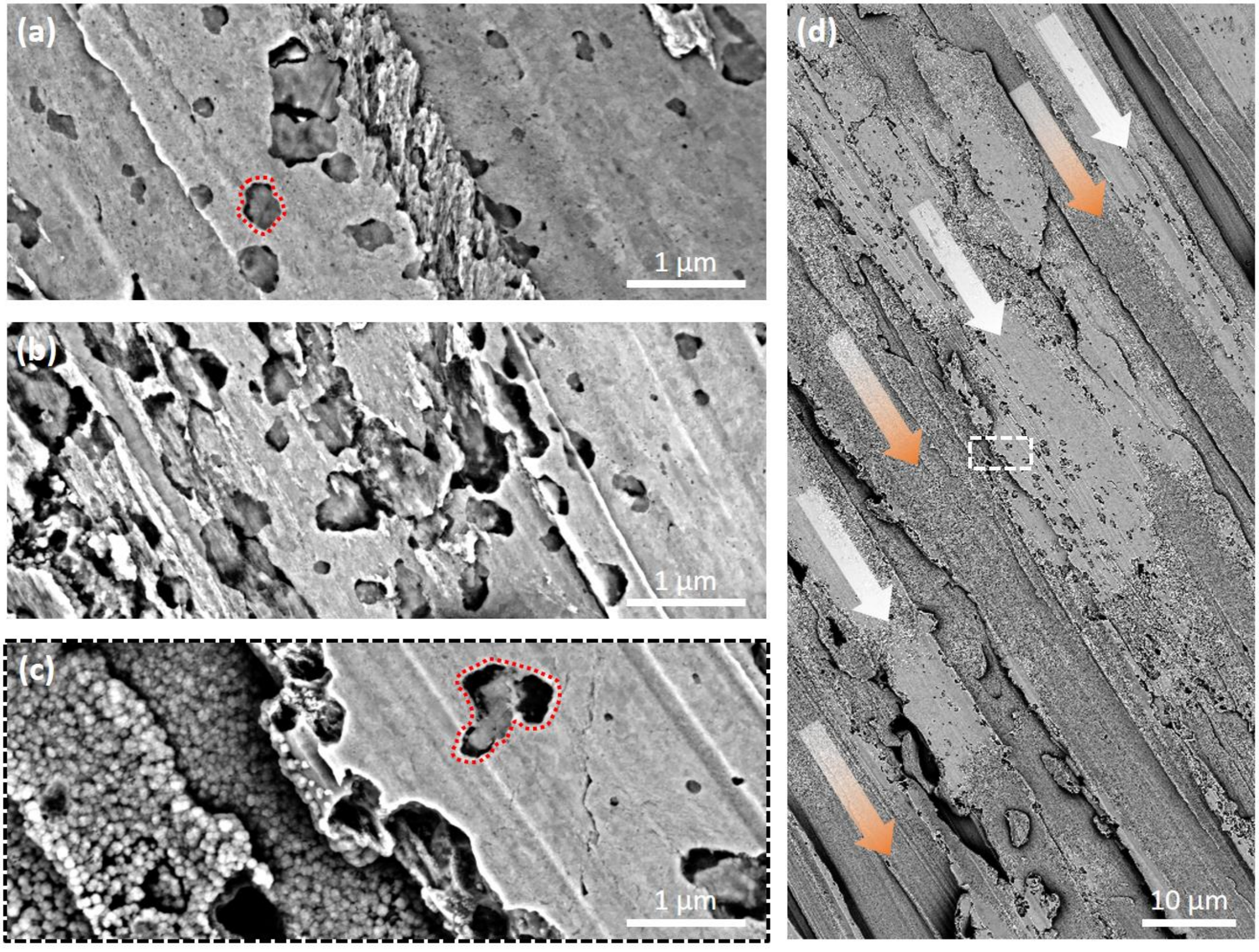

Figure 5

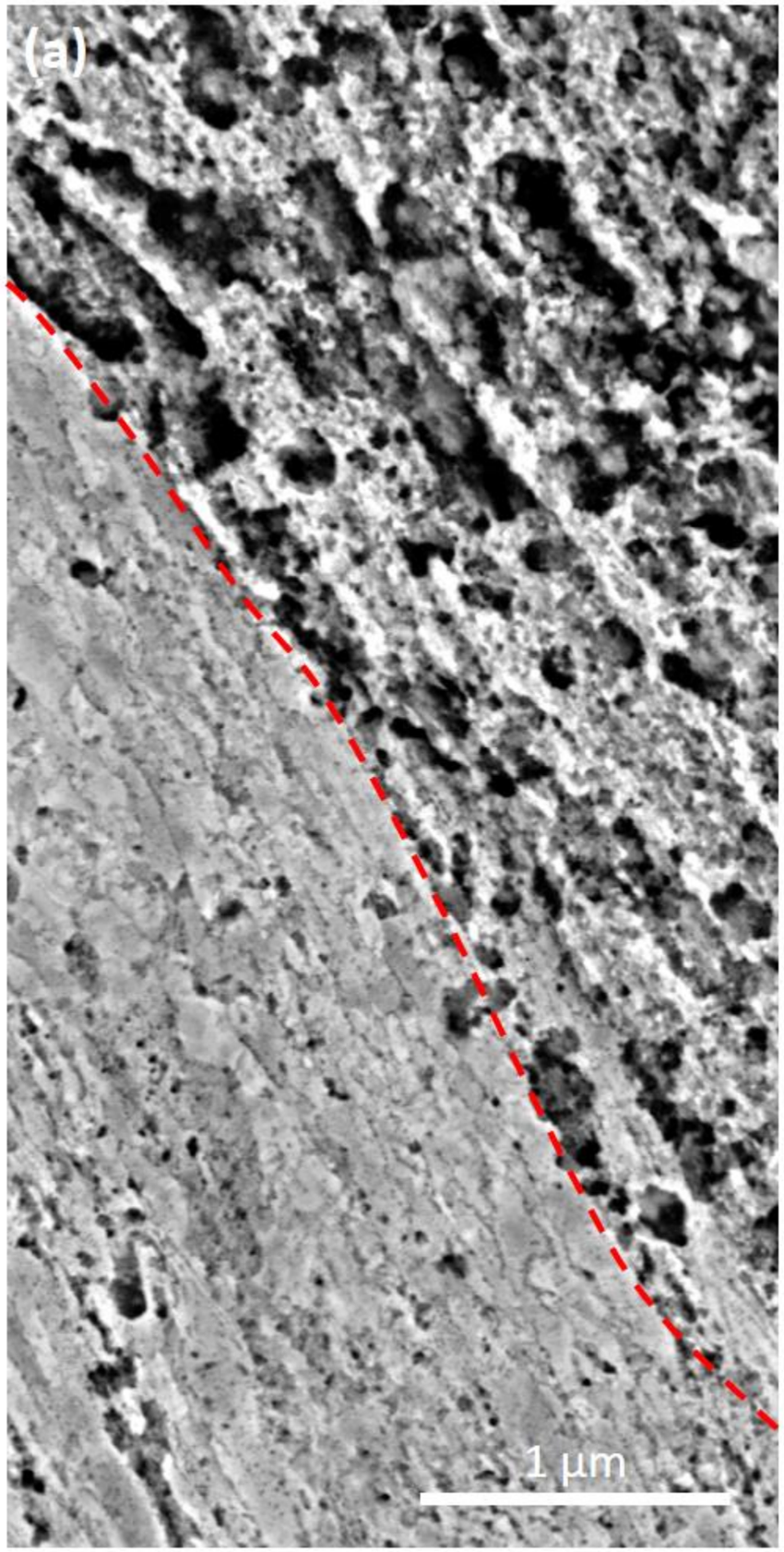

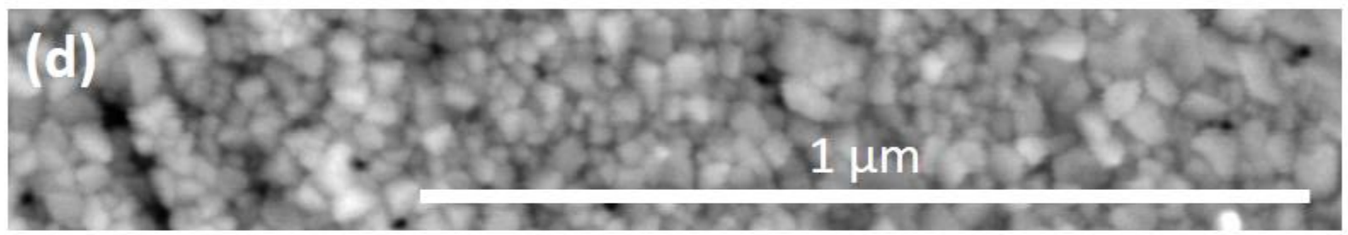

(e)

Oxide growth	Corrosion sites	0.1 X *E. coli*		1 X *E. coli*		5 X *E. coli*	
0.45% NaCl		+++	-	X	--	X	---
0.9% NaCl		++	-	X	--	X	---
1.8% NaCl		+	-	++	--	X	---

Figure 6

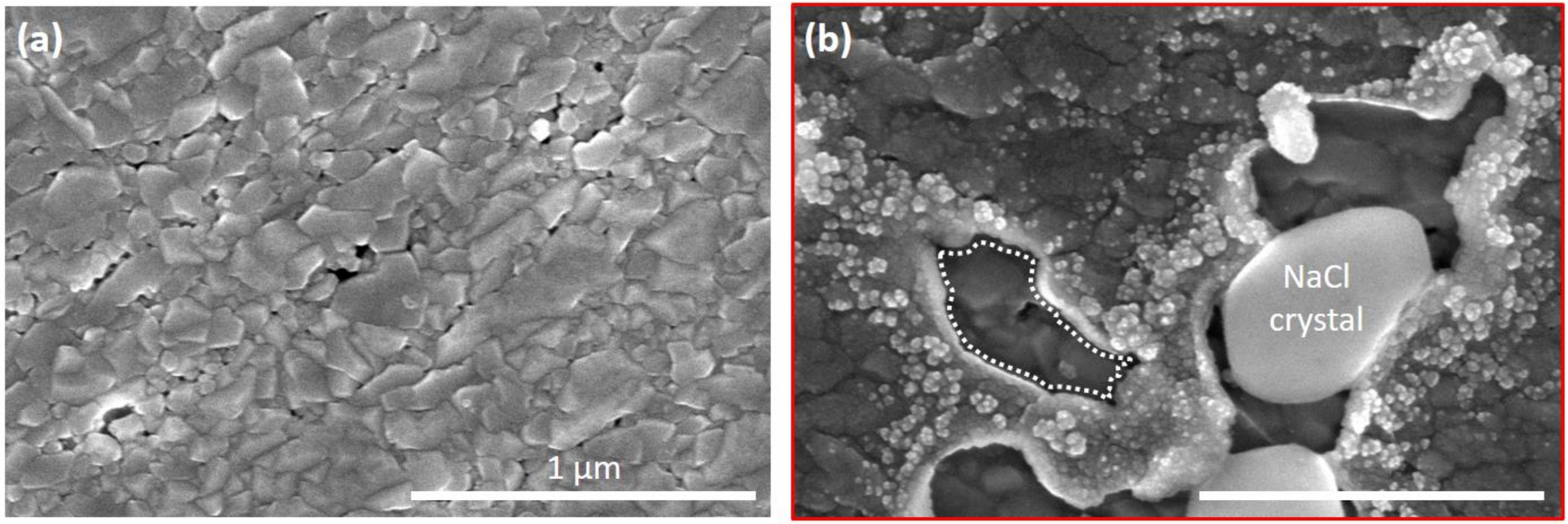
(a)
1 µm
(b)
NaCl
crystal
(c)
Intensity (counts)
e11
e10
e9
e8
e7
e6
e5
e4
e3
Cu
See caption
NaCl
Cu2O
(111)
(110)
(200)
(111)
(200)
(220)
(211)
(220)
(311)
(222)
(400)
Without cleaning
Cleaned before aging
10
20
30
40
50
60
70
80
90
100
2 Theta (°)

Figure 7

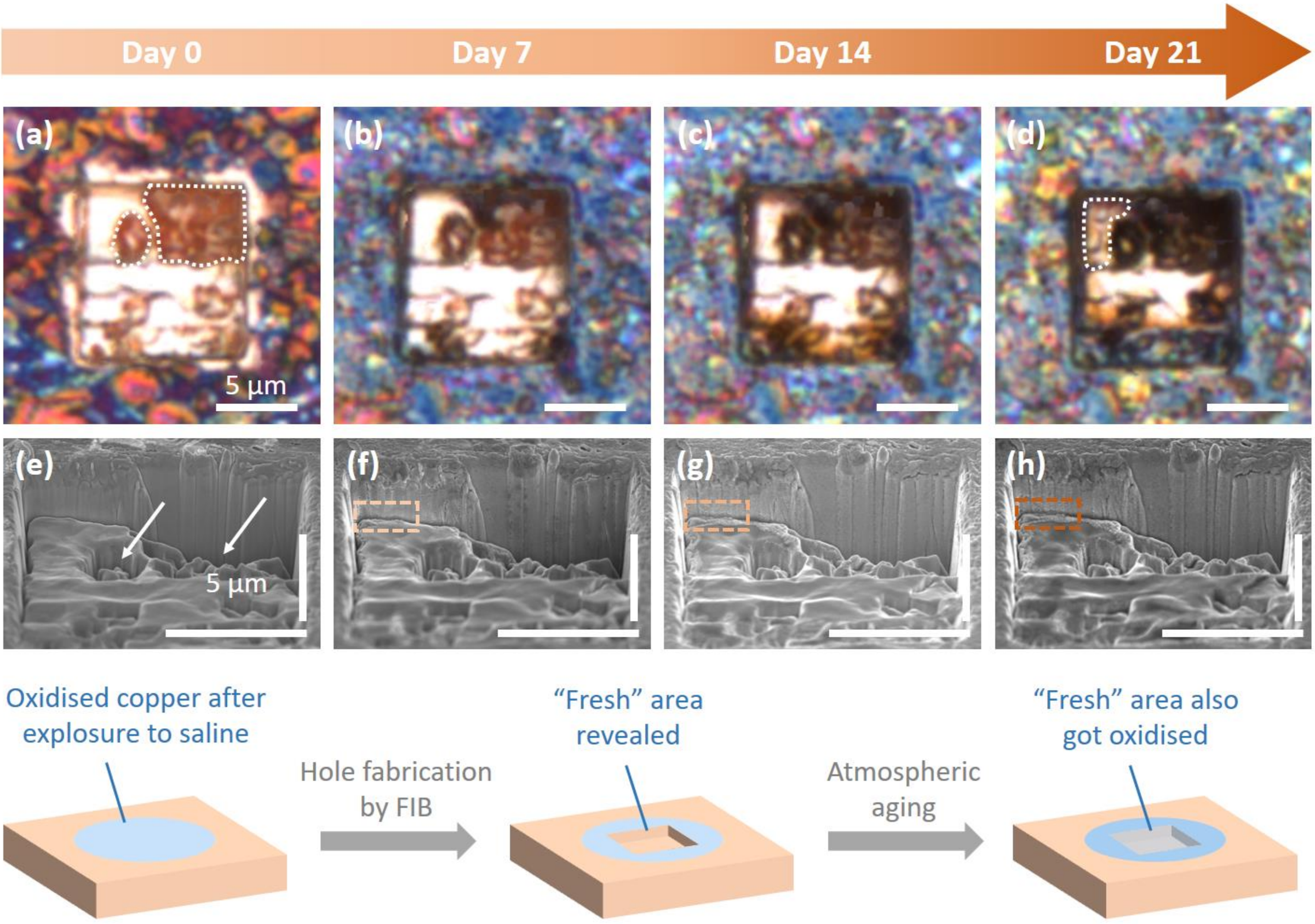
Day 0
Day 7
Day 14
Day 21
(a)
(b)
(c)
(d)
5 µm
(e)
(f)
(g)
(h)
5 µm
Oxidised copper after explosure to saline
Hole fabrication by FIB
"Fresh" area revealed
Atmospheric aging
"Fresh" area also got oxidised

Figure 8

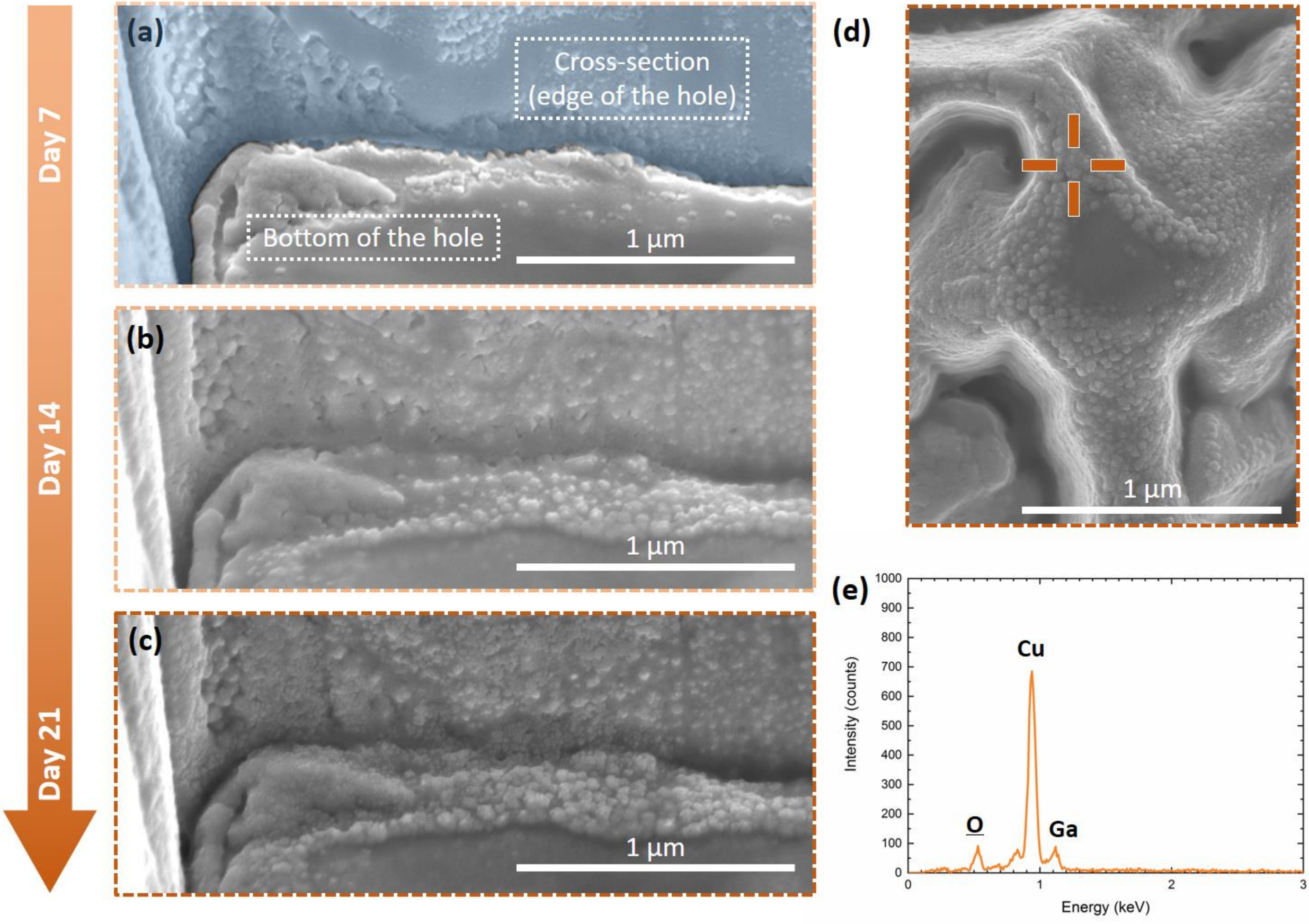
Day 7
Day 14
Day 21
(a)
Cross-section
(edge of the hole)
Bottom of the hole
1 µm
(b)
1 µm
(c)
1 µm
(d)
1 µm
(e)
Intensity (counts)
Energy (keV)
Cu
O
Ga
0
100
200
300
400
500
600
700
800
900
1000
0
1
2
3

Sodium chloride (NaCl) for copper surface

1. Assists copper release

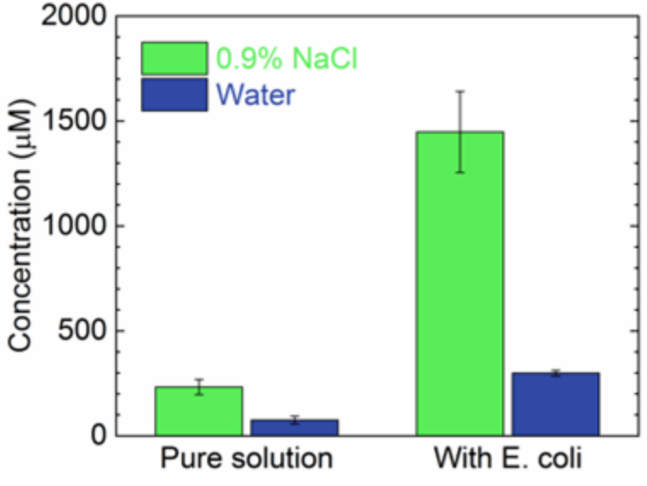

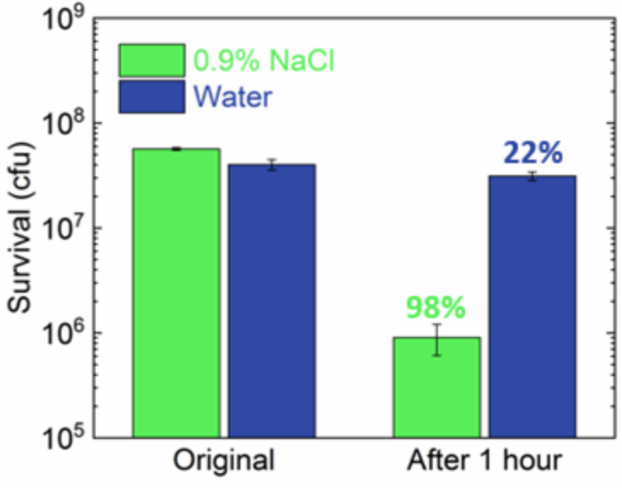

3. Introduces atmospheric corrosion

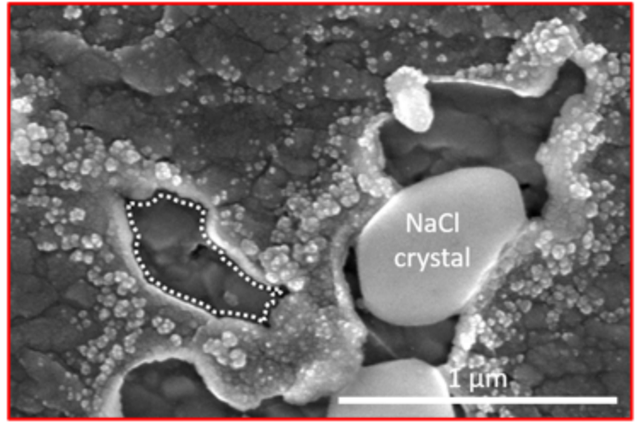

2. Enhances antibacterial efficiency